ELSEVIER

International Journal of Mass Spectrometry 221 (2002) 21–38

International Journal of Mass Spectrometry

www.elsevier.com/locate/ijms

Electron flood charge compensation device for ion trap secondary ion mass spectrometry

A.D. Appelhans*, M.B. Ward, J.E. Olson

Idaho National Engineering and Environmental Laboratory, P.O. Box 1625, Idaho Falls, ID 83415-2208, USA

Received 25 April 2002; accepted 6 August 2002

Abstract

During secondary ion mass spectrometry (SIMS) analyses of organophosphorous compounds adsorbed onto soils, the measured anion signals were lower than expected and it was hypothesized that the low signals could be due to sample charging. An electron flood gun was designed, constructed and used to investigate sample charging of these and other sample types. The flood gun was integrated into one end cap of an ion trap secondary ion mass spectrometer and the design maintained the geometry of the self-stabilizing extraction optics used in this instrument. The SIMION ion optics program was used to design the flood gun, and experimental results agreed with the predicted performance. Results showed the low anion signals from the soils were not due to sample charging. Other insulating and conducting samples were tested using both a ReO_4^- and a Cs^+ primary ion beam. The proximity of the sample and electron source to the ion trap aperture resulted in generation of background ions in the ion trap via electron impact (EI) ionization during the period the electron gun was flooding the sample region. When using the electron gun with the ReO_4^- primary beam, the required electron current was low enough that the EI background was negligible; however, the high electron flood current required with the Cs^+ beam produced background EI ions that degraded the quality of the mass spectra. The consequences of the EI produced cations will have to be evaluated on a sample-by-sample basis when using electron flood. It was shown that the electron flood gun could be intentionally operated to produce EI spectra in this instrument. This offers the opportunity to measure, nearly simultaneously, species evaporating from a sample, via EI, and species bound to the surface, via SIMS. (Int J Mass Spectrom 221 (2002) 21–38)
Published by Elsevier Science B.V.

Keywords: Secondary ion mass spectrometry (SIMS); Quadrupole ion trap; Electron flood; Sample charging; Simulation; SIMION

1. Introduction

Detection and characterization of low levels of hazardous chemicals on natural surfaces (soils, minerals, vegetation) is important for evaluating risk, developing and assessing decontamination or remediation methods, and understanding the fate and transport of chemicals in the environment. Secondary ion mass spectrometry (SIMS) has been used extensively to detect and characterize adsorbed compounds and their interactions with the matrix (soil, mineral, vegetation) [1]. Most of the matrix materials (samples) are nonconductors, and thus methods to overcome sample charging are required to apply SIMS to these samples. Uncontrolled charging of samples when performing SIMS can lead to unstable secondary ion kinetic energy distributions that reduce mass resolution and/or secondary ion collection efficiency; can defocus the

* Corresponding author. E-mail: ada2@inel.gov

1387-3806/02/$ – see front matter. Published by Elsevier Science B.V.
PII S1387-3806(02)00892-8

primary beam at the sample, blurring and distorting imaging resolution; and in general cause reduced and, in extreme cases, complete loss of signal [2–5].

In studies of a series of organophosphorous compounds adsorbed onto soils, the anion signals we measured were lower than we expected based on previous experience. It was hypothesized that the low signals could be due to sample charging, in spite of the charge-control method we were using [6]. We tested this hypothesis by designing and installing an electron flood gun on our instrument that allowed us to actively control the charge on the sample.

The degree of sample charging and its effects is mediated by the sample composition and its matrix, the electrostatic and magnetic field characteristics of the sample region, the magnitude and polarity of the primary beam, and the relative flux of positive and negative charge sputtered from the sample during bombardment. Several different methods have been used to mitigate or at least stabilize sample charging. The most common method is electron flood, in which the sample is flooded with electrons at various times during the analysis sequence to bring the sample potential to a constant level. A wide variety of approaches have been used to accommodate the specific needs of different instruments and their electrostatic and magnetic field characteristics [3,7–10]. The adverse effects associated with electron flood include the possibility of altering the sample chemistry and changes in ion mobility in the sample because of potential gradients on the surface, and damage to the molecular structure of the sample by high-energy electrons [11]. To avoid the need for electron flood and these associated adverse effects, several other methods have been explored. Conductive grids placed over the sample provide charge-carrying pathways and diminish the effects of the sample charge on the near-sample electric field, but with the obvious adverse consequences [3,12]. The use of neutral primary beams greatly reduced sample charging, but the complications of generating high-energy neutral beams with sufficient intensity and beam focusing constrained this approach [13–17]. Interleaved pulsed extraction of positive and negative secondary particles combined with a neutral or negative primary ion beam was shown to provide a measure of control and to stabilize the degree of charging [18]. A specialized geometry provided a self-stabilizing field that allowed the sample potential to self-adjust to a stable potential when using a negative or neutral primary beam [6]. The self-stabilizing field approach works with most samples, but since it depends on the sample-dependent flux of secondary ions and electrons, it cannot be actively controlled to force a sample to a specific potential. Controlling the specific level of the potential on the sample is desired because it can then be set to maximize the transport of ions to the mass spectrometer.

To optimize the collection of secondary ions in our ion trap based SIMS (IT-SIMS), the sample is located very close to one of the ion trap end cap apertures. This results in a large solid angle and reduces the path length and concomitant chance for scattering by the buffer gas. To control sample charging in this environment we developed specialized ion optics that resulted in a self-compensating field at the sample [6]. This approach works well for most samples, but relies on the inherent flux of positive and negative charge from the sample, which is dependent on sample composition. Thus while a stable sample potential can be achieved, it may not be at an optimum level for transmission of the secondary ions into the ion trap. Since both negative ions and electrons remove negative charge from the sample when sputtered, and since for many samples the flux of negative charge leaving is greater than the flux of positive charge leaving, samples can charge positive, even under bombardment with a negative primary beam. The self-stabilizing optics method provided a means to manipulate the emitted flux so that most samples could also be forced negative, allowing the extraction of negative ions. However, this method is essentially passive and does not provide a broad range of control over the level (potential) to which the sample charges. To provide a more active control of the sample potential when extracting negative ions from the sample, a means to flood the sample with low-energy electrons was required. The primary design constraints were to provide the electron flood while keeping the sample very close to the ion trap end cap and retaining the features of the self-stabilizing

optics. An electron flood gun was designed and tested that nests within the end cap region of a commercial ion trap mass spectrometer and can utilize the EI source filament power supply of the commercial instrument for operating the electron flood gun. The electrostatic and mechanical designs are described and test results are presented in the following sections, and the question "Is sample charging limiting anion detection on soil samples?" is answered.

2. Design

The goal of the design was to develop a means to inject low-energy electrons into the sample region of the IT-SIMS while maintaining the features of the self-stabilizing optics design. In the self-stabilizing optics, the sample is located 4 mm from the aperture in the ion trap end cap, and the end cap aperture is expanded to 6 mm in diameter and covered with a grid with 2 mm spacing. An ion-optical element referred to as a leakage ring [6] surrounds the sample. With this existing design as a baseline, our objective was to include the following features in the design:

- Provide the necessary flux of low-energy electrons to the sample surface in order to force the sample to a stable negative potential in the range of −5 to −25 V.
- Minimize the possibility that the electrons would result in EI ionization of gas phase species.
- Use the electron filament power supply in the mass spectrometer to operate the electron flood gun.

By stabilizing the sample potential in the −5 to −25 V range, ion transmission into the ion trap and subsequent trapping is optimized. In addition, this range implies that low-energy electrons could be used which would minimize the possibility of sample damage and EI ionization of gas phase species.

From our previous modeling of the ion trap injection optics, it was clear that the RF field from the ring electrode would penetrate some distance past the grid on the end cap and into the sample region. This added another complication to the ion optics design, as the electrostatic field will not be constant and its amplitude will be dependent upon the RF voltage level during ionization. The possible adverse effects of the penetrating RF field necessitated shielding the electron producing filament from the RF field, and giving the electrons a ballistic trajectory prior to entering the sample region that would minimize the impact of the RF field on their final trajectory to the sample. In addition, since the potential of the sample is an integral component of the electrostatic field in the sample region, and the potential on the sample could vary considerably, it was also necessary to shield (electrostatically) the electron-emitting filament from the sample. Lastly, we had to prevent electrons from leaving the electron source during certain phases of the instrument operation (ion scan out and detection). Fig. 1 shows a conceptual design of an electron flood gun nested in the ion trap end cap that meets these requirements.

2.1. Electrostatic design

The SIMION [19] ion optics modeling program was used for the electrostatic design. SIMION models were constructed that incorporated the ion trap and the sample optics region of the instrument and included a gas collision model to simulate the effects of the helium buffer gas [20]. A model using a two-dimensional cylindrical potential array with a resolution of 0.1 mm per grid-unit was used to develop the general design and investigate the effects of the RF field on the electron trajectories. Fig. 2 shows a cross section of the

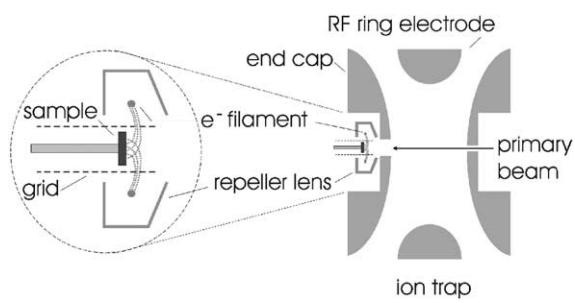

Fig. 1. Conceptual design of the electron flood gun and its position in the ion trap.

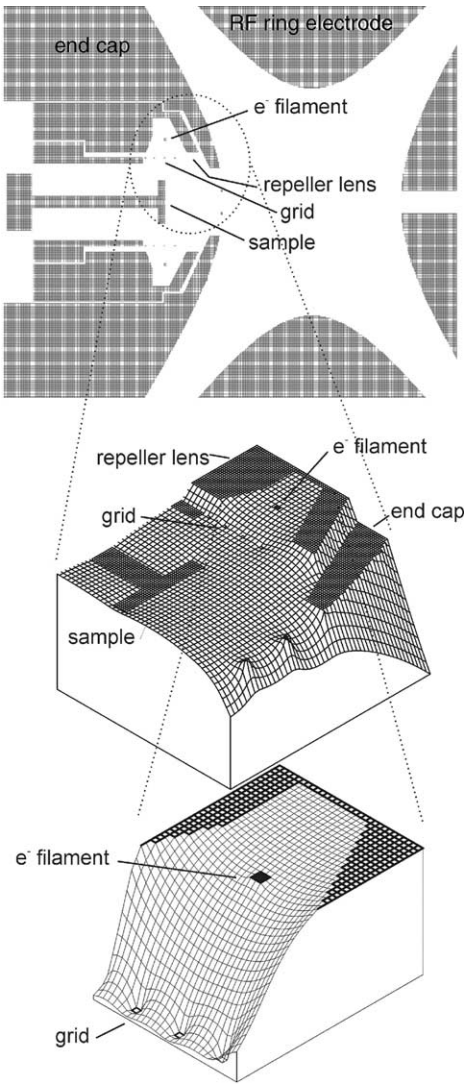

Fig. 2. Cross section view of the SIMION two-dimensional model (top) and a potential energy surface view of the sample region (middle) and the region around the filament (bottom). Voltages: RF ring, +300 V; end caps, 0 V; filament, −15 V; repeller lens, −16 V; grid, −6 V; and sample, 0 V.

model and a potential energy surface view of the model under static conditions with the RF level at +300 V. The electron flood gun consists of a shaped cylindrical cup (labeled repeller lens in Fig. 2) opened on the inside, with the filament located at approximately the center of the cup. When operating, the repeller lens is

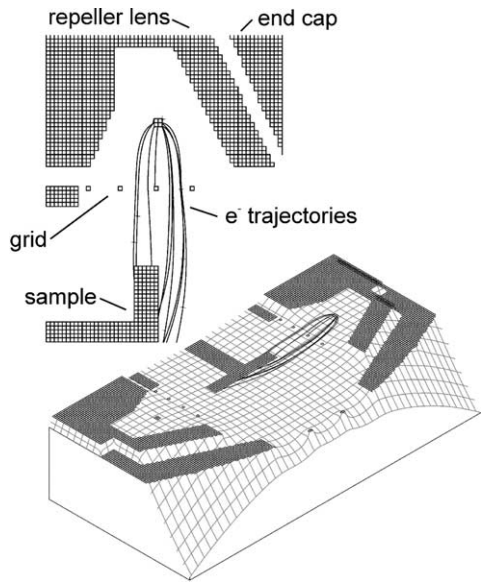

Fig. 3. Electron trajectories shown in cross section and on the potential energy surface.

at a slightly more negative potential than the filament, resulting in a shaped field that funnels the electrons emitted from the filament toward the grid. The repeller lens opens onto a cylindrical grid that surrounds the sample. This grid serves the same function as the leakage ring (see [6]) in the self-stabilizing optics method, and electrostatically isolates the electron filament from the sample. Fig. 3 shows a set of electron trajectories in cross section and on the potential energy surface (the height corresponds to the magnitude of the potential). The trajectories shown in Fig. 3 were calculated with the voltage on the ring electrode corresponding to the peak RF voltage at ∼30 amu (300 V). The filament voltage was −15 V, the repeller lens was −16 V, the grid was −6 V, and the sample and end cap were at ground.

As the electrons collect on the sample, its potential is driven negative. In theory, the maximum potential the sample can be driven to is the potential of the electron-emitting filament, since this determines the electron potential energy. Fig. 4 shows a set of electron trajectories when the filament and sample are at −15 V. None of the electrons strikes the sample, the

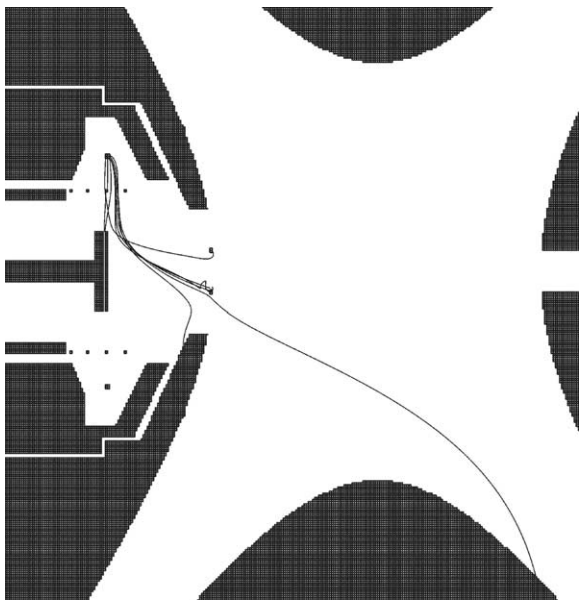

Fig. 4. Electron trajectories when the sample is at the same potential as the electron filament (−15 V), RF at 40 amu setting.

RF pulls some of the electrons into the ion trap, and most of them strike some other surface in the sample region. This demonstrates the self-limiting nature of the design; the sample charging can not get into a positive feedback loop because the electrons eventually do not have sufficient energy to reach the sample. However, there is a concern with the electrons that are diverted into the ion trap: will they result in EI ionization of residual gases, generating an unwanted (perhaps) background signal? This issue can only be investigated via actual experiment (and is discussed later).

Studies were conducted with the model to elucidate the effect of the filament position and the voltage drop along the filament on the electron flux reaching the sample. The two-dimensional SIMION model was used to investigate the effects of the position of the filament within the repeller lens, as this was anticipated to be a difficult fabrication step. The results indicated that the design was sufficiently robust to

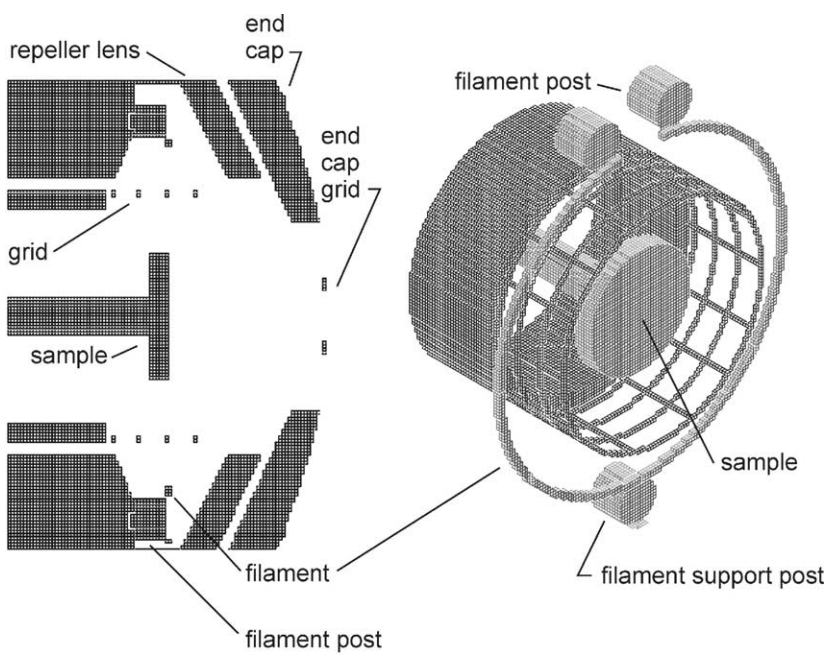

Fig. 5. Cross section and isometric view of the three-dimensional SIMION model of the electron flood gun. Scale is 0.1 mm per grid-unit.

accommodate "less than perfect" positioning of the filament and still obtain the desired electron trajectories. The results of the experimental measurements supported this conclusion, as discussed later. The modeling studies showed that the maximum electron emission was obtained when the potential difference between the filament and the repeller lens was small, only 1 V in the examples shown. Since the estimated voltage drop along the filament could be up to 3 V, the electrostatic field into which the electrons are emitted will not be uniform along the filament. To investigate the effects of this gradient, a three-dimensional model of the flood gun without the full ion trap was used. The spatial resolution of the model was maintained at 0.1 mm per grid-unit, and the filament was divided into eight regions, each set at a different potential, to simulate the voltage drop along the filament. The total drop was 3 V, resulting in a differential between each segment of 0.375 V. In the three-dimensional model, the grid was also modified to include the longitudinal as well as the radial wire segments. Fig. 5 shows a cross section view of the three-dimensional model and an isometric view of the filament, grid and sample region. Fig. 6 shows a set of electron trajectories in an isometric cut and a potential energy surface view, with the filament potential dropping from −18 to −15 V as described earlier, the repeller lens at −16 V, the grid at −6 V and the sample at ground. The trajectories show that the effects of the filament voltage drop are minor when the difference between the filament and the repeller lens is kept within 1–2 V. Given this result, the possibility of simply floating the repeller lens potential off one leg of the filament was investigated experimentally and found to work, eliminating the need for a separate voltage supply for the repeller lens. The SIMION model was used as a template for the mechanical design of the electron gun.

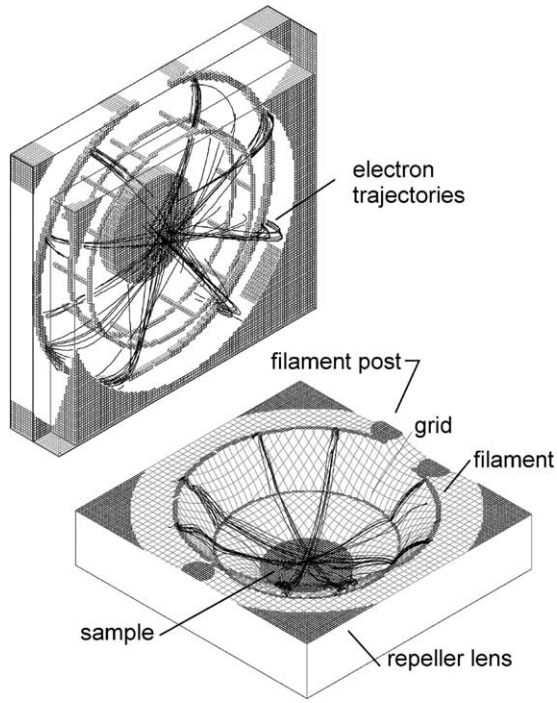

Fig. 6. Isometric and potential energy surface views of electron trajectories with 3 V drop along the filament.

2.2. Mechanical design

The ion trap SIMS uses a modified Varian Saturn 2000 mass spectrometer, previously described [21]. The flood gun electrostatic design shown in Fig. 2 was used to develop a mechanical design that would fit in the ion trap and support housing. A cross section of the mechanical design of the electron flood gun mounted in the ion trap end cap is shown in Fig. 7. Fig. 8 is a photograph of the individual components (exploded view) and the assembly. The filament is circular, with a stabilizing post located half way around the circumference. Re filament wire (0.127 mm diameter) was spot welded to post assemblies pressed into the flood gun body and electrically isolated from the repeller lens. The repeller lens components were constructed of aluminum and selected regions were anodized to provide electrical isolation. The grid was constructed of nickel mesh of 13.7 lines per inch that was spot welded to a stainless steel support cylinder pressed into the base of the repeller lens assembly. The flood gun assembly nests in the end cap as depicted in Fig. 7. The ion trap end cap has been relieved on the back side for the filament leads to pass out, the interior profile of the end cap back side has been modified to accept the

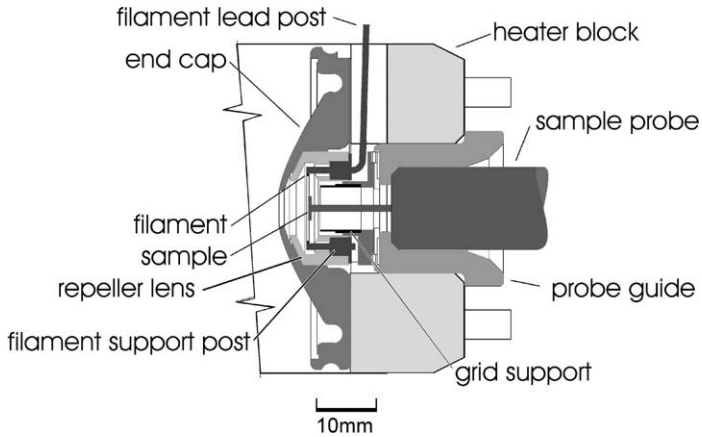

Fig. 7. Mechanical drawing of electron flood gun assembly in the ion trap heater block.

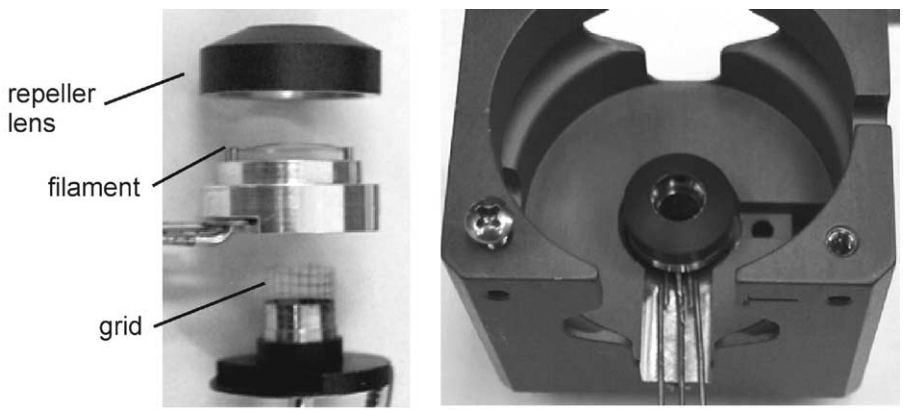

Fig. 8. Left: exploded view of the flood gun components; from the top: the repeller lens, filament assembly and the grid assembly. Right: assembly mounted in trap heater block.

flood gun assembly, and the ion trap heater block in which the entire ion trap is contained was modified to permit access to the leads. Detailed drawings of the modifications are available upon request. A description of the modifications to the Varian filament power supply necessary to operate the flood gun is given in Appendix A.

3. Experimental results

Experiments were conducted to assess the performance of the flood gun when using a negative primary beam and analyzing for negative secondary ions, to identify an optimum range of operating conditions, and to identify any adverse effects of the electron flood on the quality of the anion mass spectra. Soil samples were analyzed to answer the question: “Is sample charging limiting anion detection on soil samples?” A variety of other samples were analyzed to further characterize the utility of electron flooding. In addition, the utility of the electron flood gun for analysis with a positive primary beam and the possibility of using the electron flood gun as an EI ionization source were explored. In the experiments described later the electron flood gun was operated with a stand-alone

power supply that could be floated over a wider voltage range (than the internal filament power supply) in order to define the operating envelope.

3.1. Characterizing performance with a negative primary ion beam

3.1.1. Defining the operating envelope

Previous experience had shown that the potential on the sample could be measured directly during bombardment with the primary beam by using an appropriate electrometer [6] and a conducting sample probe. To do this, a conductive sample was attached to a conductive sample probe that was isolated from the insertion system and connected to an electrometer. As the sample charged, the sample/probe potential was measured with the electrometer. This configuration allowed both the potential (relative to ground) on the sample and the electron flux on the sample to be measured (though not simultaneously). Our standard sample mounts are number 18 steel nails to which the sample is attached using double-stick tape. However, in these experiments, a thin film of soap was rubbed directly on the nail head. This provided a well-defined anion signal from a conducting surface. With this sample the electron current striking the sample and the potential of the sample were measured as the electron flood gun settings were varied. The results showed that the sample charged to the voltage of the electron-emitting filament, and then was stable. This was expected, since once the sample reached the same voltage as the filament the electrons were no longer attracted to the sample. This is the mechanism that allows the sample voltage to be controlled (by adjusting the filament voltage).

3.1.1.1. Measured efficiency. The efficiency with which the emitted electrons reach the sample was estimated by measuring the total emitted electron current and the current striking the sample. The total emitted electron current was measured by connecting the repeller lens to the electrometer and floating them both at +9 V (to attract the emitted electrons) while holding the grid at a voltage slightly more negative than the filament (to push the electrons towards the repeller lens). The electron current striking the sample was measured by connecting the electrometer to the isolated sample probe fitted with a conducting sample. The voltages on the filament and grid were varied to find optimum voltages for two different settings on the repeller lens: one with the repeller lens set at the high leg of the filament potential, and the other with it set at the low leg of the filament potential (the voltage drop across the filament was ∼3 V). Fig. 9 shows the results of these measurements. The high leg configuration puts more electrons on the sample. From the measurements (Fig. 9) the efficiency of the system was estimated to be ∼50%. Based on our experience making these measurements we settled on a voltage for the filament between −15 and −18 V with the grid at −6 V. This provided good efficiency and coincided with previous unpublished work showing that ion injection was optimum for ions in the 15 eV range. In addition, by holding the grid at −6 V (∼12 V differential between the filament and the grid), the electron flux onto the sample was near optimum (shown later) and sputtered positive ions were inhibited.

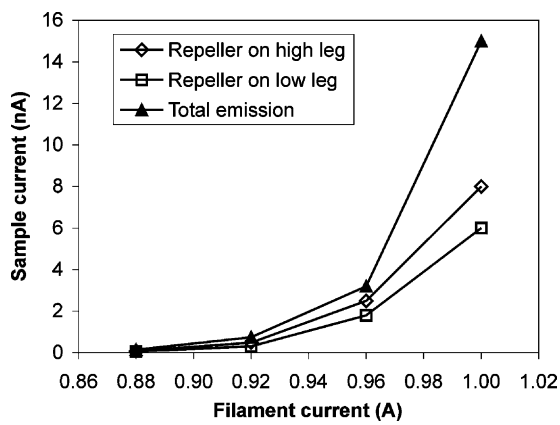

Fig. 9. Electron current measured on the sample probe with the repeller lens tied to the low leg or the high leg of the filament power supply; and the total emitted electron current measured at the repeller lens (with the repeller lens floating at +9 V) as a function of the filament current.

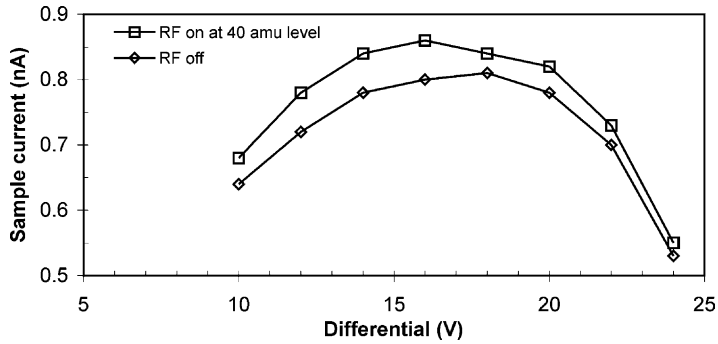

Fig. 10. Measured electron current at the sample as a function of the differential voltage between the filament and the grid with the ion trap RF on and off.

3.1.1.2. Effect of grid potential and RF level. Since the grid electrode acts as a focusing element for the electrons, its effect on the electron current reaching the sample was investigated. In addition, since the RF field projects into the grid/sample region, the effect of the RF level was also investigated. Fig. 10 shows the electron current reaching the sample as a function of the voltage differential between the grid and filament for two cases: with the RF set at the 40 amu level and with the RF turned off. It is clear that the RF field is not keeping the electron current from reaching the sample; in fact, the RF field seems to slightly increase the electron current on the sample. Within the range 12–22 V differential (Fig. 10), the electron current on sample is relatively insensitive to the voltage differential between the grid and filament.

3.1.1.3. Tracking electron injection into the ion trap. Some of the electrons will be injected into the ion trap, particularly as the sample reaches its final potential (Fig. 4). Since we wanted to minimize the number of electrons injected into the ion trap, some means to determine this was needed. Tracking the electrons injected directly into the trap experimentally is extremely difficult. However, the filament was constructed from Re wire, and when heated above ~1200 K produces ReO_4^- ions in low abundance. Since in electrostatics, charged particle trajectories are independent of mass (nonrelativistic conditions), the ReO_4^- ions and electrons emitted from the filament will behave identically; thus, the ReO_4^- ions provide a probe for evaluating electron behavior. Indeed, ReO_4^- ions were observed in the anion mass spectrum when the electron-emitting filament was on and the ion trap was configured to trap and detect anions. Measurements of the trapped ReO_4^- signal as a function of the voltages on the filament and the grid showed that there was a distinct range over which the ReO_4^- ions were directed into the trap, and that there was a range that excluded it. The question was: Did the range of grid potentials that was optimum for directing electrons onto the sample overlap the range that directed ReO_4^- (and by association, electrons) into the trap? Fig. 11 shows the trapped ReO_4^- signal and the electron current measured on sample (from Fig. 10) as a function of the differential voltage between the filament and the grid. The signals have all been normalized to the maximum within each data set. The results show that the injection of ReO_4^- (and electrons) is strongly dependent on the differential voltage between the filament and the grid, but that the range over which they are injected is relatively narrow, and does not overlap the region where the electron current on sample is maximum. Thus by operating the filament and grid at a potential difference of 10 V or greater the electron current on sample can be maximized and the ReO_4^- (and, by inference, electron current) injected into the ion trap, minimized.

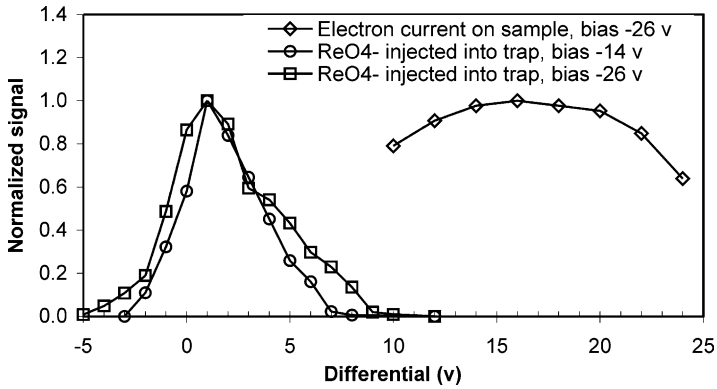

Fig. 11. The trapped ReO_4^- signal at two filament voltages as a function of the voltage differential between the filament and the grid (left, squares and circles); and the measured electron current on the sample as a function of the voltage differential between the filament and the grid (right, diamonds, from Fig. 10.)

3.1.2. Charging rate and equilibrium potentials

All of the previous measurements were made under essentially static conditions, that is, the primary beam was not bombarding the sample. However, during SIMS analysis, the situation is dynamic, and the rates of electron and primary ion flux become important. In the absence of a primary beam, the rate at which the sample charges is a function of the capacitance of the sample (and probe, in this case) and the flux of electrons. Fig. 12 shows the sample potential as a function of time, starting with the sample at 0 V and with an electron current on the sample of 0.38 nA (as measured with the sample grounded). The response is approximately logarithmic; as the sample potential increases, the sample becomes less of a potential well and fewer electrons are attracted to it. (Note that the charging rate will be much faster when the sample is isolated electrostatically from the probe.)

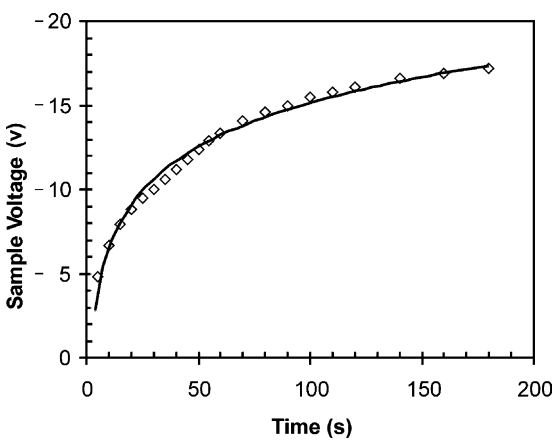

Fig. 12. Sample potential as a function of time after the electron flood is turned on, and a logarithmic function fit to the data.

During bombardment of the sample with the primary beam, the electron flood gun is competing with the sputtering process, which is (usually) causing electrons (and ions) to be ejected from the sample. At the same time, the primary beam is bringing charge into the sample. Thus, the potential on the sample will be unstable unless these terms balance. When the sample is initially bombarded, its potential begins to change based on the incoming and outgoing charge. The change in sample potential causes a change in net charge flux, either in a negative feedback mode (leading to stability) or a positive feedback mode (leading to instability); the reader is referred to [6] for a detailed discussion of this process. If a stable potential is achieved, it can be at a level that is less than optimum for transmission of the sputtered ions into the ion trap, either because it is too low (ions do not have adequate energy to enter the trap) or too high (ions have too much energy and pass through the trap). As an illustration, Fig. 13 presents the measured sample potential (normalized to the filament potential), and the associated intensity of the *m*/*z* 97 anion as a function of the

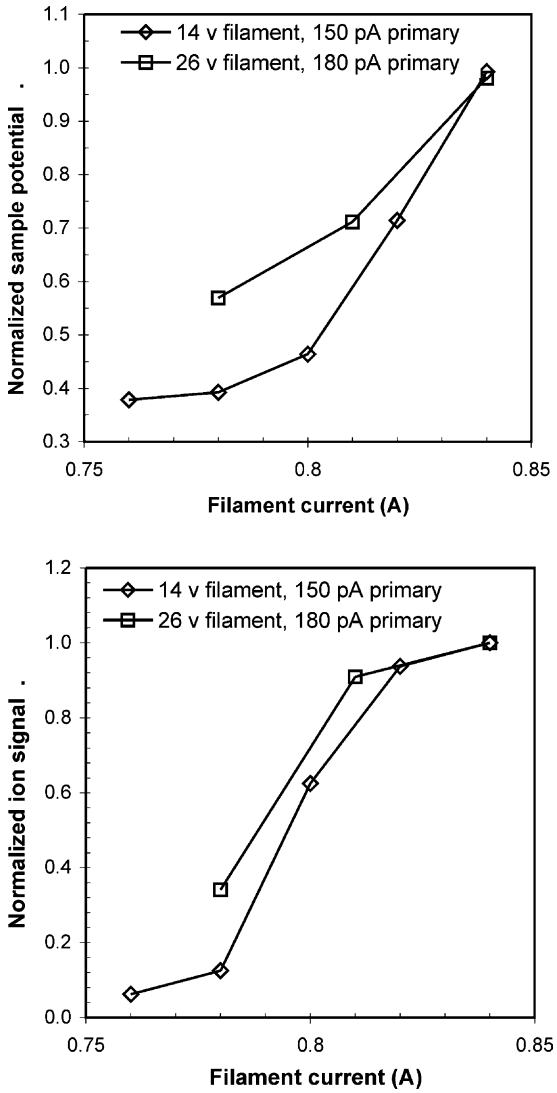

Fig. 13. Measured sample potential normalized to the filament potential (top) and the *m*/*z* 97 anion signal (bottom), normalized to the maximum signal, for two different settings, as a function of the electron-emitting filament current.

filament current (and by implication the electron current). The *m*/*z* 97 anion, corresponding to HSO_4^-, is the base peak in the anion spectrum of the soap film applied to the sample planchette. At a given filament (electron) current the sample came to an equilibrium potential and a stable *m*/*z* 97 signal could be measured; however, if this equilibrium potential was not at the optimum level, the transport of ions into the trap was compromised. So, for example, even though the sample potential had reached an equilibrium at 0.8 A filament current (Fig. 13, top), the trapped signal intensity was only 60% of the signal attained with a 0.84 A filament current (which produced a more negative equilibrium sample potential). Again, while these static measurements illustrate the behavior, the process is actually dynamic.

The dynamics are illustrated by the dependence of the measured ion signal on the bombardment time (during which ions are being sputtered from the sample, referred to hereon as the ionization time). If the electron flood current was insufficient, that is, more electrons were being lost to sputtering than were coming in, the sample slowly charged in the positive direction, reducing anion transmission. Under these conditions, the increase in anion signal with ionization time was not constant (1:1 proportional); Fig. 14 illustrates the effect. The measured *m*/*z* 97 anion signal is shown as a function of the ionization time at three different electron flood current levels. When the electron flood current was high enough to maintain the sample potential throughout the ionization period, then the ion signal increased proportionally with the ionization time, as occurs for the 0.84 A example. However, for

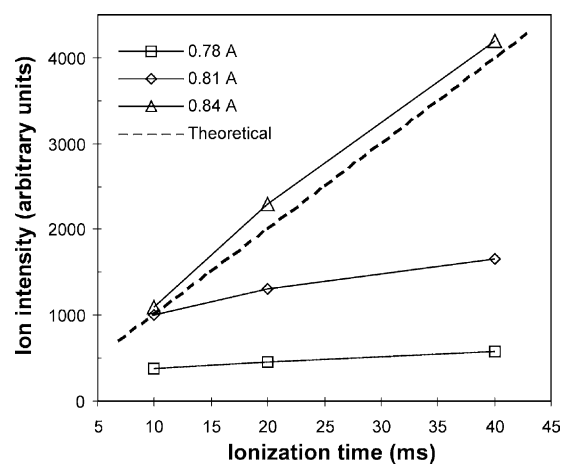

Fig. 14. Measured *m*/*z* 97 anion signal as a function of ionization time for three different electron flood current levels, and the theoretical response curve.

the 0.78 and 0.81 A levels, the electron flood current was insufficient, the sample did not hold an optimum potential, and as the ionization time was increased the ion signal fell behind. This illustrates that the sample potential was undergoing a dynamic change during the ionization time. During these measurements, the electron flood was on during both ionization and the ion scan out. Thus during the ion scan out segment (in which the primary beam was turned off) the sample was driven negative by the electron flood and was at the optimum potential when ionization first began. Nevertheless, as the period progressed, the total negative charge ejected from the sample was greater than the electrons coming in, driving the sample potential in the positive direction. Note that for the 0.78 A case the electron current at even the shortest ionization time was insufficient. All of these measurements were made with the conductive sample on the floating sample probe and thus the time constants were much longer than for a typical insulating sample; however, the same processes were occurring, just at a different rate. For an isolated sample, a ∼10 nA electron flood current was necessary to maintain a stable and optimum potential on floating metal samples (worse case because of their low work function and thus high electron yield) using a 180 pA ReO_4^- primary ion beam.

3.1.3. Effects of EI derived ions

As the sample reaches the equilibrium potential it no longer attracts the electrons and many of the electrons are diverted into the ion trap and could potentially produce cations via EI. This could cause space charge peak broadening or could result in unwanted ion–ion reactions. To investigate these issues the instrument was configured to detect cations while the injection optics were configured to inject anions. Fig. 15 shows (a) the anion mass spectrum of a soap film on stainless steel, (b) the cation mass spectrum with the electron flood and the primary beam on, and (c) with the electron flood on and primary beam off. The spectrum with the electron flood off but the primary beam on showed no signal (as expected since the insertion optics were set for anion insertion). Fig. 15 shows there was an abundant EI spectrum, and for this sample, it was clear that the trap contained many more cations than anions. For the sample shown here, the anion spectrum was unchanged (except in intensity) with the flood gun on or off, indicating that the presence of the cations produced by EI in the trap did not compromise the composition of the anion signal.

In other cases, the cations generated by EI ionization degraded the quality of the anion mass spectra. Peak broadening and diminished intensity were observed for samples that required long ionization times, clear evidence of space charge. The degradation could be removed and the anion intensity increased by applying selective ion storage during ionization, thus greatly reducing the number of stored cations and resultant space charge. The consequences of the EI produced ions will have to be evaluated on a sample-by-sample basis when using electron flood.

3.2. Analysis of soil and other sample types

A variety of sample types were tested to determine whether electron flood could improve the anion signal level and stability and whether sample composition was a significant parameter. The sample types included soil, metal oxides, metal powders, metal foils (electrically isolated), and vegetation.

3.2.1. Soil and metal oxides

For the soil and metal oxides (alumina and silica), which are all nonconductive materials with high work function surfaces, electron flood was not needed to achieve an optimum sample potential when analyzing for anions. Fig. 16 shows the anion mass spectrum of pinacolyl methylphosphonic acid (PMPA) on soil with and without electron flood, there was essentially no difference. These results imply that either the sample charged to the optimum voltage without the need for additional negative charge (electrons) or that the sample charged to a negative voltage that was higher than optimum (and which can not be changed via electron flood). The later possibility was discounted based on two observations: (1) When the grid voltage was set to +5 V, the anion signal went to zero. Modeling and experience with the floating probe assembly

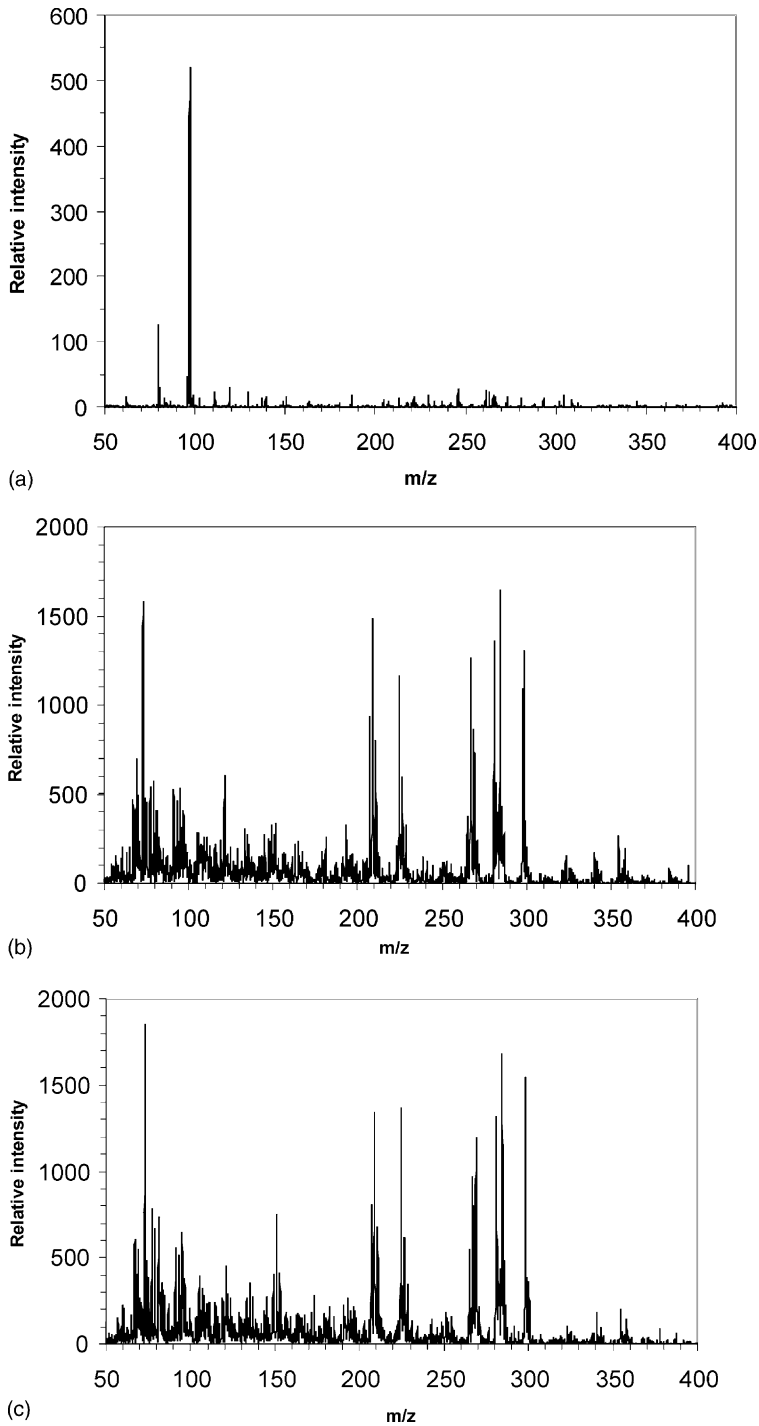

Fig. 15. (a) Anion SIMS spectrum of soap film with electron flood and primary on. (b) Cation SIMS spectrum of soap film with electron flood and primary on. (c) Cation spectrum from soap film with electron flood on, primary off.

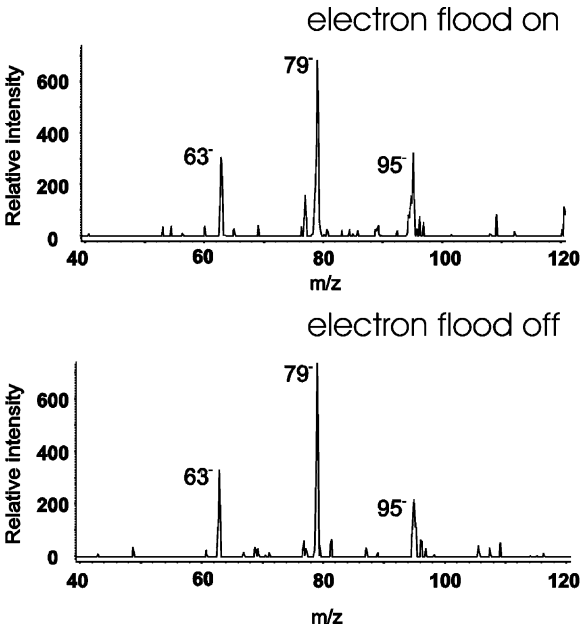

Fig. 16. SIMS spectra of fragment ions from PMPA on soil with (top) and without (bottom) electron flood.

showed that if the sample was charged more negative than ∼−2 V, the anions would be injected into the trap despite the +5 V on the grid. If the sample was charged less negative than ∼−2 V, then the sputtered ions were attracted to the grid and were not injected into the ion trap. Thus the loss of signal with a grid voltage of +5 V indicated the sample was not charged negative by more than ∼−2 V. (2) By incrementally increasing the filament voltage from −10 to −40 V, and thus driving the sample voltage to the same level, the anion signal was observed to drop, as expected, because as the ion kinetic energy increased to 40 eV the ion trapping efficiency decreased. Thus, it was concluded that the low anion signals from soil samples were implicit to the sample–analyte combination, and were not the result of sample charging; answering the posed question: Is sample charging limiting anion detection on soil samples? The metal oxides (alumina and silica) showed the same behavior, the signals could not be enhanced with electron flooding. This implied that the loss of electrons from these high work function surfaces was small enough that the incoming ReO_4^- beam combined with the self-stabilizing optics design was able to keep the sample at the required potential.

3.2.2. Metal foils and metal powders

In contrast to the behavior observed for soils and metal oxides, when analyzing metal foils and powders, materials with low work function surfaces, the loss of electrons was too high, and the addition of electrons with the flood gun greatly improved the anion signal level and stability. Fig. 17 shows the isotope peaks of ReO_3^- and ReO_4^- anions sputtered from Re powder on double-stick tape (top), and the HSO_4^- peak in the anion spectrum of a soap film on stainless steel foil (attached with double-stick tape, and thus electrically floating), with and without electron flood. Peak intensities increased by an order of magnitude for these samples when using the electron flood. This clearly demonstrated that the electron flood process worked, when required.

3.2.3. Vegetation

The electron flood filament heats up the sample region and thus the samples after they are introduced. The sample heating will increase the release of semivolatile species from the sample, which could impact the quality of the mass spectra if the concentration were high enough and resulted in an increased production of cations from EI ionization, or simply too high a pressure. In samples such as soils, metal powders, and ceramic powders, we have not seen any significant issues arise. However, when analyzing fresh cut samples of plant leaves, which we have done routinely in the ion trap SIMS for many years [1,22], we found that when the flood gun was operated the temperature in the sample region was too high, causing background pressures in the 5×10^{-5} Torr range, too high for producing quality mass spectra. This problem could be overcome to a degree by turning the electron flood filament on only for brief periods when needed, but this results in a less stable electron emission current. Fortuitously, our previous experience has shown that the self-stabilizing optics design [6] of the insertion lens maintains the vast majority

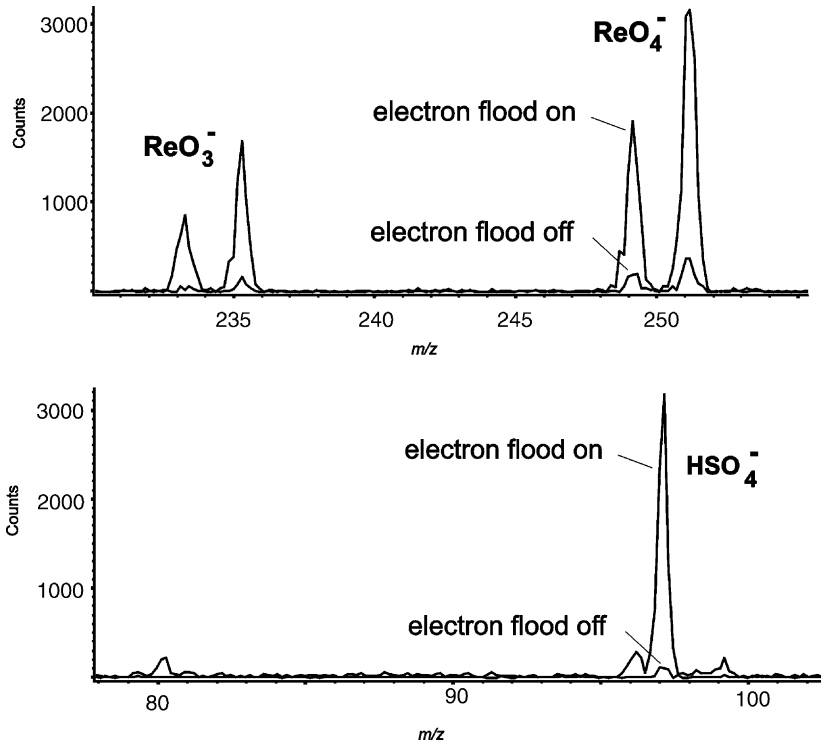

Fig. 17. Measured anion peaks for Re metal powder (top) and a soap film (bottom) on stainless steel sheet using ReO_4^- primary beam with and without electron flood.

of vegetation samples at an acceptable potential for anion analysis.

3.3. Application with a positive primary ion beam

Controlling sample charging is even more challenging when using a positive primary ion beam, since the additional positive charge brought to the sample by the primary beam exacerbates the charging. To evaluate the application of this flood gun with a positive primary beam the ReO_4^- source was replaced with a Cs^+ source operated at 3 kV and ~200 pA. Samples of Re metal powder, Teflon tape, soil spiked with phosphonic acids, powdered $Al(OH)_3$, soap films on stainless steel, and ammonium salts on stainless steel were analyzed. The results were mixed, the flood gun was able to maintain charge stability on all of the samples during cation analysis, but was only successful for anion analysis on the Re powder and soap film samples. Note that without the flood gun it was not possible to get even cation spectra for any of these samples. A very weak anion spectrum was obtained from the soil, but it required an electron flood current of several microamperes. The problems resulting from EI ionization of background gases remained and would have to be monitored in practice.

3.4. EI ionization

Since the electron flood gun was located at one of the ion trap end caps, and provided a beam of low-energy electrons, a natural question was: Could it be used for EI ionization? In the role of an electron flood gun, it was intended to be used primarily when collecting anion SIMS spectra. As an EI source, it would be employed for producing cation spectra. Using PFTBA calibration gas as a sample, the filament and grid potential were varied to find a level that

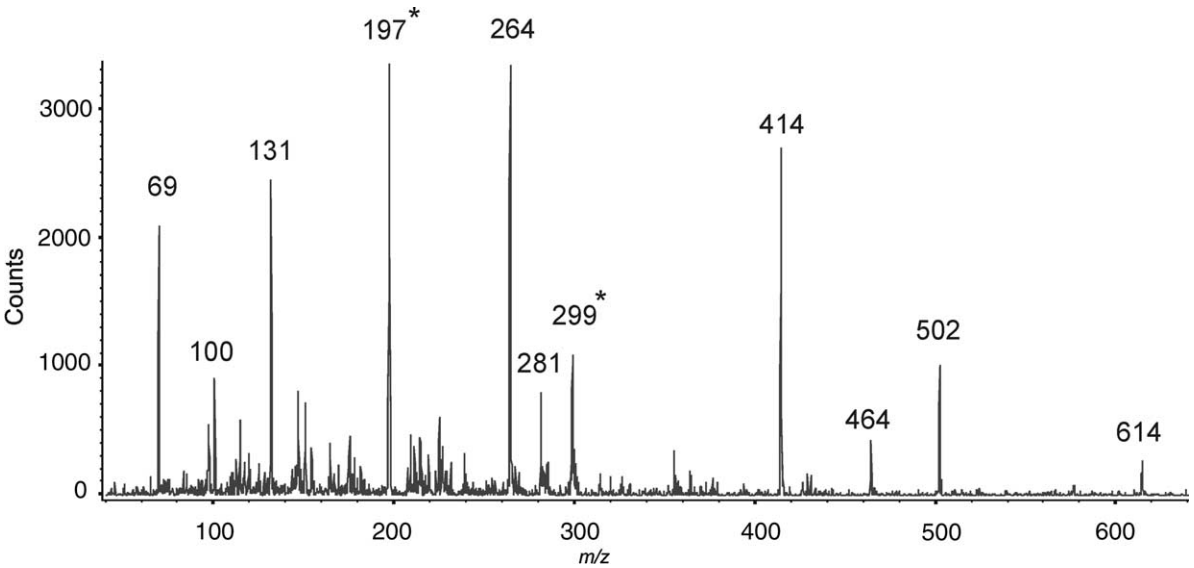

Fig. 18. EI spectrum of PFTBA calibration compound produced with electron flood gun; starred peaks are unidentified contaminants.

optimized the EI ion signal (note that the SIMS samples were not inserted during these measurements). Fig. 18 shows the EI spectrum of PFTBA acquired with the filament at −60 V and the grid at −56 V with an electron current on the order of 60 nA (about a factor of 100 less than is typically used in GCMS applications of this instrument). This is a reasonable spectrum, all of the major PFTBA peaks, with the exception of *m*/*z* 219, are present in good abundance. This spectrum was acquired with the ion trap at ∼30 °C, a base pressure of $\sim 2 \times 10^{-7}$ Torr, 6 ms ionization time with calibration gas pressure of 7×10^{-6} Torr and a helium pressure of 3×10^{-5} Torr. The data in Fig. 11 indicated that the optimum voltage differential between the grid and the filament for injecting electrons into the ion trap was 1–2 V, close to the conditions of Fig. 18. This implies that the ions were being formed inside the trap, as opposed to in the sample region just outside the trap. When the grid voltage was set to the values (based on the modeling) that keep the electrons in the "sample" region, the EI signal was very poor. Thus, we concluded that the EI ions were being formed in the ion trap. If the residual background was adequately clean, it should be possible to produce EI spectra of species evaporating from a sample, and then analyze the surface of the sample via SIMS.

4. Conclusions

It was hypothesized that sample charging was reducing the ion trap SIMS anion signal for organophosphorous compounds adsorbed onto soil. To test this hypothesis an electron flood gun was designed, constructed and tested; and soil samples were analyzed with and without applying an electron flood. The results showed that the low anion signals from the soil samples were not due to sample charging. The flood gun was integrated into one end cap of a commercial ion trap, could be operated with the filament power supply of the commercial ion trap mass spectrometer, and maintained the geometry of the existing self-stabilizing ion extraction optics. The SIMION ion optics program was used to design the flood gun, and experimental results agreed with the predicted performance. In addition to soils, other insulating and conducting samples were tested using both a ReO_4^- and a Cs^+ primary ion beam. Samples with low work functions (metal powders on double-sided tape) which

charged positive and could not be analyzed for anions under ReO_4^- primary ion bombardment without use of the electron flood, could be analyzed when using the electron flood gun. Samples with high work functions (ceramics, polymers, soil) were shown to not charge positive under ReO_4^- primary ion bombardment and could be held at a suitably negative potential during anion extraction with the self-stabilizing optics without use of the electron flood gun. When using the Cs^+ primary beam, the electron flood gun was able to maintain charge stability on all of the samples during cation analysis, but was only successful for anion analysis on ungrounded metal samples. The insulating samples required higher than acceptable levels of electron current to maintain charge stability under anion extraction conditions when using the Cs^+ primary beam. The proximity of the sample and electron source to the ion trap aperture results in generation of background ions in the ion trap via EI ionization during the period the electron gun is flooding the sample region. When using the electron gun with the ReO_4^- primary beam, the required electron current was low enough that the EI background was negligible; however, when a high electron flood current was required then the background ions produced via EI degraded the quality of the mass spectrum. The consequences of the EI produced ions will have to be evaluated on a sample-by-sample basis when using electron flood. It was also shown that the electron flood gun could be intentionally operated to produce EI ionization spectra in this instrument, offering the opportunity to concurrently produce EI spectra of species evaporating from a sample and analyze the surface of the sample via SIMS (for nonvolatile components).

Appendix A. Varian Saturn 2000 filament supply modifications

In order to drive the electron flood gun from the Varian Saturn 2000 electronics, the emission regulator for the trap filament had to be disabled and the power supply reconfigured so that it was in a current regulating mode. The trap filament power supply is located on the power board, which is the large circuit board located behind the SAP board. The instrumentation amplifier, AR4, which is an Analog Devices 620A, provides the control feedback for the emission regulator. Its input is taken across a 1 kΩ resistor, R99, the gain is set for 25 and this corresponds to a feedback signal with a proportionality of −2.5 V per 100 μA of emission current. A maximum of 100 μA of electron emission current is controlled from an 8-bit DAC giving a resolution of 0.392 μA. R69 (5 W 0.25 Ω) is in series with the filament and the voltage drop across it is used to drive the over current protection circuit. R69 also provides a convenient place to extract the new feedback signal necessary to control the filament current. The new feedback signal has a proportionality of −2.5 V per 10 A of filament current and has a resolution of 0.0392 A.

The procedure for reconfiguring the power supply for current regulation is to first remove AR4 and solder an IC socket onto the board. Insert a new AD620A instrumentation amplifier in the socket with pins 1, 2 and 3 bent out and not inserted into the socket. This removes the feedback necessary for emission regulation and configures the amplifier to have unity gain. Jumpers need to be soldered from pin 2 of AR4 to the right side of R69 and from pin 3 to the left side of R69. This provides the new feedback signal to control the filament current.

The original circuit was designed as an emission regulator and the control loop had been properly tuned to give the appropriate response. No attempt has been made to retune the control loop to optimize the response for filament current regulation. Therefore, care must be taken when turning on and adjusting the filament current to ensure that the step change is not too large to cause overshoot of the filament current, which could destroy the filament.

References

[1] G.L. Gresham, G.S. Groenewold, J.C. Ingram, A.D. Appelhans, D.A. Dahl, J.E. Olson, J.E. Delmore, J. Process Anal. Chem. 4 (2001);

G.L. Gresham, G.S. Groenewold, A.D. Appelhans, J.E. Olson, M.T. Benson, M.T. Jeffery, B. Rowland, M.A. Weibel, Int. J. Mass Spectrom. 208 (2001) 135;
G.S. Groenewold, A.D. Appelhans, J.C. Ingram, G.L. Gresham, A.K. Gianotto, Talanta 47 (1998) 981;
J.C. Ingram, A.D. Appelhans, G.S. Groenewold, Int. J. Mass Spectrom. Ion Processes 175 (1998) 253;
J.C. Ingram, G.S. Groenewold, A.D. Appelhans, J.E. Delmore, J.E. Olson, D.L. Miller, Environ. Sci. Technol. 31 (1997) 402;
J.C. Ingram, G.S. Groenewold, A.D. Appelhans, D.A. Dahl, J.E. Delmore, Anal. Chem. 68 (1996) 1309;
J.C. Ingram, G.S. Groenewold, A.D. Appelhans, J.E. Delmore, Anal. Chem. 67 (1995) 187.

[2] R. Jede, O. Ganschow, U. Kaiser, in: D. Briggs, M.P. Seah (Eds.), Practical Surface Analysis, Vol. 2, Wiley, New York, 1992, p. 96.

[3] A. Benninghoven, F.G. Rudenauer, H.W. Werner, in: Secondary Ion Mass Spectrometry, Wiley, New York, 1987, p. 882.

[4] A.D. Appelhans, Int. J. Mass Spectrom. Ion Processes 88 (1989) 161.

[5] G.J. Leggett, J.C. Vickerman, App. Surf. Sci. 84 (1995) 253.

[6] D.A. Dahl, A.D. Appelhans, Int. J. Mass Spectrom. Ion Processes 178 (1998) 187.

[7] B. Hagenhoff, D. van Leyen, E. Niehuis, A. Benninghoven, J. Vac. Sci. Technol. A 7 (1989) 3056.

[8] A.J. Eccles, J.C. Vickerman, J. Vac. Sci. Technol. A 7 (1989) 234.

[9] H.N. Migeon, M. Schuhmacher, G. Slodzian, Surf. Interface Anal. 16 (1990) 9.

[10] R.T. Short, M. McMahon, W.M. Holland, P.J. Todd, J. Am. Soc. Mass Spectrom. 5 (1994) 37.

[11] D. Briggs, A.B. Wootton, Surf. Interface Anal. 4 (1982) 109.

[12] H.W. Werner, N. Warmoltz, J. Vac. Sci. Technol. A 2 (1984) 726.

[13] A.J. Eccles, J.A. van den Berg, A. Brown, J.C. Vickerman, J. Vac. Sci. Technol. A 4 (1986) 1888.

[14] J.A. van den Berg, Vacuum 36 (1986) 981.

[15] F. Degreve, J.M. Lang, Surf. Interface Anal. 7 (1985) 177.

[16] A.D. Appelhans, J.E. Delmore, D.A. Dahl, Anal. Chem. 59 (1987) 1685.

[17] J.E. Delmore, A.D. Appelhans, R.E. Shomo II, D.A. Dahl, Biomed. Environ. Mass Spectrom. 16 (1988) 237.

[18] A.D. Appelhans, J.E. Delmore, D.A. Dahl, Anal. Chem. 62 (1990) 1679.

[19] D.A. Dahl, Int. J. Mass Spectrom. 200 (2000) 3.

[20] A.D. Appelhans, D.A. Dahl, Int. J. Mass Spectrom. 216 (2002) 269.

[21] G.S. Groenewold, A.K. Gianotto, J.C. Ingram, A.D. Appelhans, Curr. Top. Anal. Chem. 1 (1998) 73.

[22] J.E. Delmore, A.D. Appelhans, Biomed. Environ. Mass Spectrom. 20 (1991) 237.